THE UNIVERSITY of EDINBURGH

# Edinburgh Research Explorer

# Toxic properties of microsome-associated alpha-synuclein species in mouse primary neurons

OPEN ACCESS
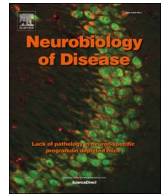
# Toxic properties of microsome-associated alpha-synuclein species in mouse primary neurons

Emanuela Colla[a,\*], Giulia Panattoni[a], Alessio Ricci[a], Caterina Rizzi[a], Lucia Rota[a], Nicola Carucci[a], Verdiana Valvano[a], Francesco Gobbo[a], Simona Capsoni[a], Michael K. Lee[b,c], Antonino Cattaneo[a,d]

[a] Bio@SNS Laboratory, Scuola Normale Superiore, Pisa, Italy
[b] Department of Neuroscience, University of Minnesota, United States
[c] Institute for Translational Neuroscience, University of Minnesota, United States
[d] Neurotrophins and Neurodegenerative Diseases Laboratory, Rita Levi-Montalcini European Brain Research Institute, Rome, Italy

## ARTICLE INFO

## ABSTRACT

α-synuclein (αS) is a small protein that self-aggregates into α-helical oligomer species and subsequently into larger insoluble amyloid fibrils that accumulate in intraneuronal inclusions during the development of Parkinson's disease. Toxicity of αS oligomers and fibrils has been long debated and more recent data are suggesting that both species can induce neurodegeneration. However while most of these data are based on differences in structure between oligomer and aggregates, often preassembled *in vitro*, the *in vivo* situation might be more complex and subcellular locations where αS species accumulate, rather than their conformation, might contribute to enhanced toxicity. In line with this observation, we have shown that αS oligomers and aggregates are associated with the endoplasmic reticulum/microsomes (ER/M) membrane *in vivo* and how accumulation of soluble αS oligomers at the ER/M level precedes neuronal degeneration in a mouse model of α-synucleinopathies. In this paper we took a further step, investigating the biochemical and functional features of αS species associated with the ER/M membrane. We found that by comparison with non-microsomal associated αS (P10), the ER/M-associated αS pool is a unique population of oligomers and aggregates with specific biochemical traits such as increased aggregation, N- and C-terminal truncations and phosphorylation at serine 129. Moreover, when administered to murine primary neurons, ER/M-associated αS species isolated from diseased A53T human αS transgenic mice induced neuronal changes in a time- and dose-dependent manner. In fact the addition of small amounts of ER/M-associated αS species from diseased mice to primary cultures induced the formation of beads-like structures or strings of fibrous αS aggregates along the neurites, occasionally covering the entire process or localizing at the soma level. By comparison treatment with P10 fractions from the same diseased mice resulted in the formation of scarce and small puncta only when administered at high amount. Moreover, increasing the amount of P100/M fractions obtained from diseased and, more surprisingly, from presymptomatic mice induced a significant level of neuronal death that was prevented when neurons were treated with ER/M fractions immunodepleted of αS high molecular weight (HMW) species. These data provide the first evidence of the existence of two different populations of αS HMW species *in vivo*, putting the spotlight on the association to ER/M membrane as a necessary step for the acquisition of αS toxic features.

## 1. Introduction

Accumulation of α-synuclein (αS) aggregates in intracellular proteinaceous inclusions called Lewy Bodies (LB) or Lewy neurites, according to their subcellular location, is a classical hallmark of Parkinson's disease (PD) and α-synucleinopathies (Goedert et al., 2012). αS is a small, soluble acidic protein highly expressed throughout the nervous system and with a well-described presynaptic localization (Iwai et al., 1995; Maroteaux et al., 1988). Point mutations in the αS gene (Appel-Cresswell et al., 2013; Krüger et al., 1998; Lesage et al., 2013; Polymeropoulos et al., 1997; Zarranz et al., 2004) and gene amplifications (Chartier-Harlin et al., 2004; Singleton, 2003) have been found in family pedigrees affected by autosomal dominant, early onset PD, although αS neurotoxicity contributes to both genetic and sporadic

---

forms of PD (Shulman et al., 2011).

Aggregation of αS in insoluble inclusion is a complex nucleation reaction that includes at least two key steps: the transition from an unfolded monomer which has a naturally intrinsic unfolded conformation [(Burré et al., 2013; Chandra et al., 2003; Fauvet et al., 2012; Theillet et al., 2016; Weinreb et al., 1996), although lately these data have been questioned (Bartels et al., 2011; Dettmer et al., 2015; Wang et al., 2011)] to an oligomer-type of structure and the transition to an insoluble β-sheet rich protofibril (Cremades et al., 2012; Deleersnijder et al., 2013). Many variables are thought to influence these transitions: point mutations, such as those associated with genetic PD (Conway et al., 1998); C-terminal truncation (Li et al., 2005); protein level and stability (Li, 2004); environmental factors (Uversky et al., 2002); post-translational modifications, such as ubiquitination, phosphorylation, nitration/oxidation (Oueslati et al., 2010).

Membrane interaction appears to be another condition that can influence formation of αS fibrils (H.-J. Lee et al., 2002). In fact, αS is believed to shift between a free and a membrane-bound state in a dynamic equilibrium with the membrane-bound state accounting for 10–15% of the total protein amount. αS can bind synaptic vesicles and its binding is believed to mediate its synaptic function (Burré, 2015). αS has been implicated in a broad range of presynaptic functions that includes binding and promoting SNARE complex assembly to favor docking of synaptic vesicles to the cell membrane (Burré et al., 2010, 2014), lipid transport and metabolism (Golovko et al., 2005, 2009), neurotransmitters release and brain plasticity (Bendor et al., 2013). Association with membranes is mediated by αS N-terminal seven 11-amino-acids repeats that are predicted to form an amphipathic α-helix. αS has been found to bind high-curvature membranes such as in presynaptic vesicles, through the acquisition of a multimeric structure with a defined orientation (Burré et al., 2014). Thus, under normal conditions αS can shuffle between a native unfolded structure to a multimeric vesicle-bound conformation at the presynaptic terminals. However it is not clear how the transition from these native conformations to a toxic type of aggregates occurs.

We have recently described the presence of toxic αS high molecular weight (HMW) species (oligomers and aggregates) associated with the endoplasmic reticulum/microsomal vesicles (ER/M) *in vivo*, in diseased Prp-A53T transgenic (Tg) mice (Colla et al., 2012a). αS HMW species were sensitive to protease degradation suggesting that these αS species were associated with the microsomal membrane on the cytosolic side. Importantly, the appearance of αS oligomers at the ER/M level temporally preceded the onset of neurodegeneration and ER stress-induced cell death in a Tg mice, suggesting the microsomal membranes might be a unique place to foster the accumulation of toxic species of αS (Colla et al., 2012b).

In this paper we took a deeper look into the ER/M-associated αS HMW species, comparing them to the rest of αS aggregates purified through low speed centrifugation. Our findings provide evidence of the existence of a toxic species of αS *in vivo*, associated with the ER/M vesicles that has unique biochemical traits and is more aggressive in spreading and inducing cell death in neuronal primary cultures.

## 2. Materials and methods

### 2.1. Animal models

Transgenic mice expressing human A53T αS under the control of the mouse prion protein (PrP) promoter [line *G2-3(A53T)*] have been described previously (Colla et al., 2012a, 2012b; M. K. Lee et al., 2002; Li et al., 2005; Martin et al., 2006). This model develops fatal neurological disease at ∼12 months of age which rapidly progresses to end state within 14–21 days of onset. Diseased mice show a drastic reduction in motor function, accumulation of intracellular αS inclusions and neuronal death. For this study, sick mice at 12–14 months of age, presymptomatic mice at 9 months and age-matched nTg littermates were

used. Presymptomatic animals did not show any motor dysfunction or αS pathology in the central nervous system. All animal studies were approved and complied in full by the national and international laws for laboratory animal welfare and experimentation (EEC council directive 86/609, 12 December 1987 and Directive 2010/63/EU, 22 September 2010).

### 2.2. Membrane fractions preparation

Membrane pellet fractions were obtained as previously described (Colla et al., 2012a). Briefly, fresh tissues were homogenized in a 1:10 (wt/vol) volume of lysis buffer (250 mM sucrose, 20 mM HEPES, 10 mM KCl, 1.5 mM MgCl$_2$, 2 mM EDTA, protease and phosphate-inhibitors cocktails) using a Teflon pestle homogenizer. Initial homogenates were centrifuged at $1000 \times g$ to remove nuclei and unbroken cells. The resulting supernatant was centrifuged at $10,000 \times g$ for 20 min at 4 °C to obtain the first membrane pellet (called P10), while the supernatant was centrifuged at $100,000 \times g$ for 1 hr at 4 °C to obtain the microsomal pellet (called P100). Both pellet fractions were washed with homogenization buffer once and centrifuged again at the same speed as previously mentioned. P10 and P100 were then resuspended in 200 or 100 μl of lysis buffer, respectively, and their protein content was determined.

### 2.3. Western blot

Immunoblot and dot blot analyses were performed as previously described (Colla et al., 2012a, b). The following antibodies were used: syn1 (1:5000; BD Transduction Laboratories, Franklin Lakes, NJ); LB509 (1:5000; Abcam, Cambridge, MA); mouse pser129-αS (1:1000; DAKO, Glostrup, Denmark), syn303 (1:1000; Biolegend, San Diego, CA); A11 (ThermoFisher Scientific, Eugene, OR). Quantitative analysis of immune detected bands was done using ImageLab Software (Bio-rad, Hercules, CA).

### 2.4. Primary hippocampal and cortical neurons preparation and P10 and P100 fractions treatment

Primary neuronal cultures were prepared from wild-type (WT) newborn (P0) hippocampus and cortex of mouse strain B6.129, according to a procedure by Beaudoin et al., (2012). Hank's Balanced Salt Solution was used as mechanical dissection medium. Tissues mechanically dissected were treated with 0.1% trypsin for 7 min at 37 °C and then collected with regular DMEM medium containing fetal bovine serum (FBS) and DNase. Preparations were centrifuged at 1000 rpm for 5 min and pellet was resuspended in Neurobasal medium containing 2% B27, 1X Glutamax, 6 mg/ml glucose, 10% FBS, 12.5 μM glutamate and 1X Gentamicin. Dissociated neurons were plated on poly-D-lysine coated coverslips placed in 24 well dishes at a concentration of about 100,000 cells/cm$^2$. At day *in vitro* (DIV) 1 the medium was replaced with new fresh Neurobasal medium containing 2% B27, 1X gentamicin and 1X Glutamax. At DIV2, 1/3 of the medium was removed and replaced with fresh medium containing 2.5 μM cytosine arabinoside for 48 hrs to reduce glial contamination.

Neurons were treated at DIV7 with 0.5, 1 or 2 μg of various pellet fractions according to the experiment. To avoid sample variability, 4–5 pellet fractions isolated from different mice with the same phenotype were pooled. For internalization experiments, neurons were fixed after 2 days, 1 week or 2 weeks of treatment.

### 2.5. Cell lines

Human neuroblastoma SH-SY5Y cells were transfected with a pcDNA3.1 plasmid carrying human WT αS cDNA tagged at the C-terminal with Myc. Cells stably carrying the plasmid were kept polyclonal and routinely cultured in DMEM medium containing 10% FBS,

1% penicillin/streptomycin and 500 μg/ml of G418 as selection antibiotic.

For pellet fractions treatment, 50,000 cells/well were plated on poly-ᴅ-lysine coated coverslips placed in 24 well dishes. The day after, pellet treatment was done following the same protocol described for neurons except that, in case of SH-αS-Myc WT, 5 μg of various membrane fractions were added. Cells were fixed after 2 days of treatment.

### 2.6. Confocal immunofluorescence

Cells were fixed with 2% paraformaldehyde and 5% sucrose solutions for 15 min at room temperature (RT) and permeabilized with 0.3% Triton x-100 (Tx-100). Standard immunofluorescence was performed as previously described (Colla et al., 2012a). The following antibodies were used: syn1 (1:2500), rabbit pser129-αS (EP1536Y, 1:1000, Abcam, Cambridge, MA), Map2 (1:10000, Abcam) and Lamp1 (1:1000, Abcam), NeuN (1:1000 Millipore, Merck, Darmstadt, Germany); syn303 (1:1000), Tau (1:10000 Synaptic system, Goettingen, Germany), mouse αS (1:200 Cell Signal, Leiden, The Netherlands).

Quantitative analysis of total fluorescence, after background subtraction or particles count per field was done using Image J software.

For the "two-stages" immunofluorescence, live cultures were incubated before fixation with 3% FBS for 30 min at 4 °C with gentle rocking and then incubated with primary antibody dissolved in 3% FBS for 30 min at 4 °C. Cells were then washed, fixed and stained following the standard procedure. Stacked images were acquired with a laser scanning confocal microscope SP2 system (Leica Microsystems) using a 63 × objective.

### 2.7. Tunel staining

After fixation, neuronal cultures were incubated with 1X Terminal Deoxynucleotidyl Transferase (TdT) Buffer (3 mM trizma base, 14 mM cacodylate sodium, 0.1 mM cobalt chloride, pH 7.2) for 15 min at 37 °C and subsequently with TdT reaction mixture containing TdT buffer, 1 mM Biotin-16-dUTP, 400 U/μl terminal deoxynucleotidyl transferase [Roche, Indianapolis, IN] for 1 hr at 37 °C. After incubation, the enzyme activity was blocked by washing with 2X Saline-sodium citrate (SSC). Unspecific binding sites were blocked by incubating for 30 min with a blocking solution containing 1% BSA and 0.1% Tx-100 at RT. Neurons were incubated with 1:3000 Streptavidin Alexa Fluor® 568 conjugate (ThermoFisher Scientific), for 1 hr at RT in the dark. After incubation, neurons were washed repeatedly with PBS and standard immunofluorescence protocol for NeuN antibody and DAPI staining was carried out.

Pictures were taken using Nikon Eclipse E600 epi-fluorescence microscope (Nikon Corp, Tokyo, Japan) with 20 × objective. Cell counting was done using ImageJ software (National Institute of Health).

### 2.8. Immunodepletion

Immunodepletion of αS species was performed by incubating 20 μg of P100 fractions (pooled from 4 mice) obtained from SpC of diseased and presymptomatic animals, with 500 ng of A11, Syn1 or Syn303 antibodies previously conjugated with protein A/G agarose (ThermoFisher Scientific). After 1 hr incubation at 4 °C, samples were centrifuged at low speed (2500 rpm for 5 min) to remove immunoprecipitated complex conjugated with the agarose. The supernatant that represented the immunodepleted sample was carefully removed, avoiding any agarose contamination. 2 μg of each sample was then loaded on a denaturing SDS Page and immunoblotted with Syn1 antibody to check for αS levels. According to the experiment 1 or 2 μg was then administered to neuronal cultures.

### 2.9. Statistical analysis

All values are expressed as the mean ± SD. Differences between means were analyzed using Student's *t*-test and one-way ANOVA followed by Tukey multiple comparisons test (Prism, Graph Pad Software, LaJolla CA).

## 3. Results

### 3.1. Biochemical characterization of αS aggregates

Because we recently identified αS oligomers and aggregates associated with the ER/M membrane in presymptomatic and diseased transgenic mice (Colla et al., 2012a, b), we decided to focus on the biochemical and functional characterization of these aggregates to understand whether distinct populations of αS HMW species exist at the same time in neurons. To do this we isolated all the αS HMW species from a disease-affected area such as the spinal cord (SpC) of sick A53T transgenic (Tg) mice and separated them into two different populations according to their sedimentation rate. These populations were named P10 and P100. P10 represents a crude membrane pellet fraction that sediments at $10,000 \times g$, containing the majority of αS aggregated species (M. K. Lee et al., 2002; Li et al., 2005) and is rich in mitochondria and synaptosomes. P100 is the microsomal pellet, a fraction that sediments at $100,000 \times g$ and is rich in ER, Golgi and synaptic vesicles. According to this protocol, there are virtually no aggregates that remain in the cytosol after centrifugation (Colla et al., 2012a). In order to correlate changes in αS compositions in different fractions to the onset of αS-driven pathology, P10 and P100 fractions were also obtained from SpC of presymptomatic (aged 9 months) mice and from pathology-free regions like cortex (Ctx) of diseased age-matched littermates.

Since C- and N-terminal truncations of the αS protein are thought to be involved with aggregation and neuronal toxicity (Li et al., 2005), we mapped the accumulation of truncated species in P10 and P100 using an antibody raised against the central portion of the protein, the NAC domain (Syn1 clone 42). Analysis of truncation showed how accumulation of the most abundant truncated fragments Syn12, Syn10 and Syn8 changed with disease onset within the two aggregates populations (Fig. 1). In presymptomatic mice, increased accumulation of Syn12, the most abundant and normally occurring C-terminal truncated fragment (Li et al., 2005), was only found in P10. With disease onset, however, the whole truncation pattern dramatically changed and P100 showed increased protein truncation compared to P10, with an elevated accumulation of all the truncated fragments analyzed, including Syn8, the aggregation-specific N- and C-terminal truncated specie. Analysis of Ctx from diseased mice, a region not affected by αS pathology in this mouse model, showed a puzzling truncation pattern with a decreased accumulation of Syn12 in P100 and concomitant increased of Syn10. No Syn8 accumulation was found in presymptomatic or Ctx from diseased mice confirming lack of aggregation in these two areas.

Thus the αS species associated with P100 show an increase in αS truncation compared to P10 that is temporally and spatially linked to the disease onset and concurrent with αS aggregation.

Since western blot analysis showed differences in the content of αS HMW bands between P10 and P100 from sick SpC, we determined the amount of αS oligomers and aggregates accumulated within the pellet fractions using specific markers of aggregation such as syn303 antibody, specific for oxidized/aggregated αS and A11, specific for oligomer species. Dotblot analysis confirmed previous data that only affected tissues in diseased mice accumulated aggregated αS (Supplemental Fig. 1), although P100 immunoreactivity to syn303 was significantly higher than in P10. Moreover P100 from sick SpC contained more αS oligomers compared with P10 as detected by the A11 that were also present in some of the P100 fractions of presymptomatic mice and more phosphorylated αS at serine 129, compared to P10, with
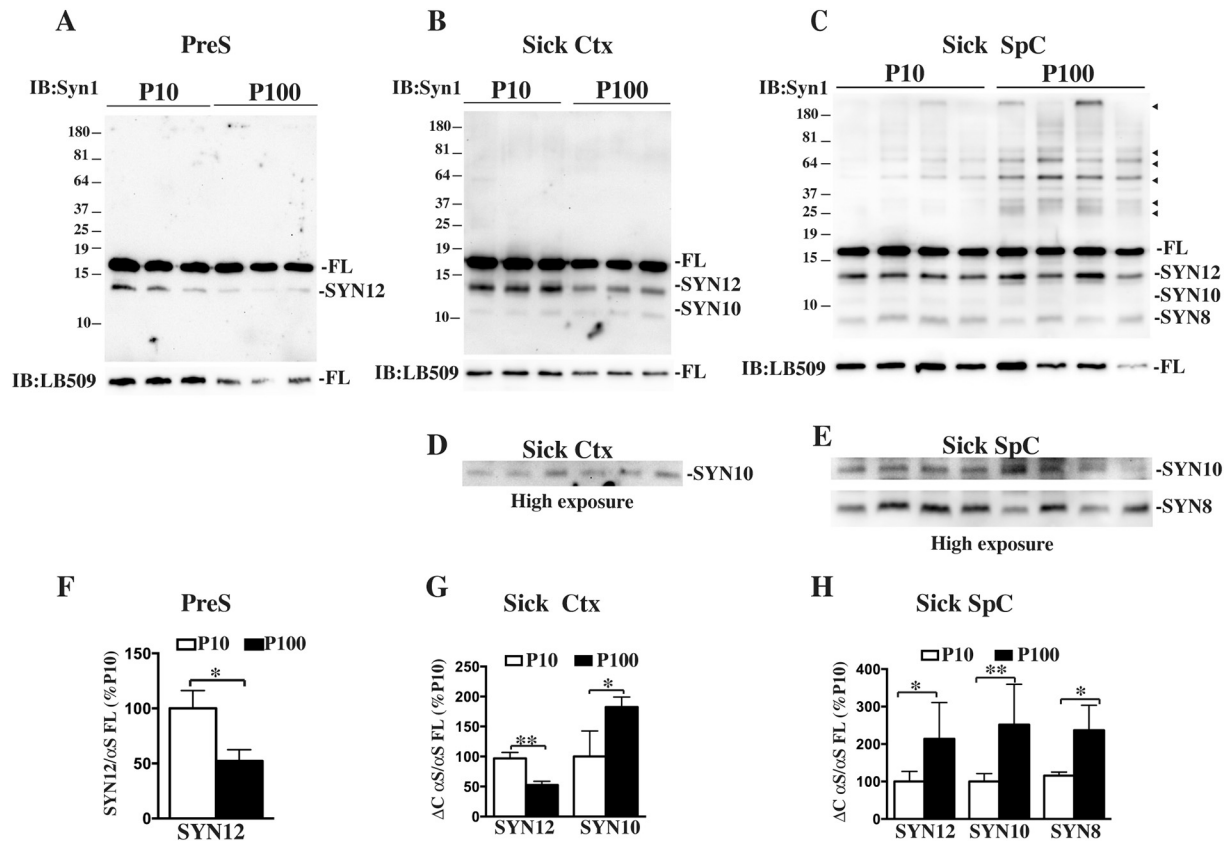
**Fig. 1.** Accumulation of αS truncated fragments in P10 and P100 pellet fractions.
**A**, **B**, **C**, Immunoblotting showing how neurodegeneration affects the levels of αS truncated fragments in P10 and P100 fractions obtained from SpC of presymptomatic (PreS) (A) or sick Ctx (B) and SpC (C) of A53T Tg mice. 2 μg of each fractions was run on a denaturing SDS-Page, transferred and blotted with syn1 antibody that recognizes the most abundant truncated fragments, Syn12, Syn10, Syn8 and HMW species (arrows heads) of αS. Human αS monomer was visualized with human specific antibody LB509. FL, αS full length monomer. **D**, **E**, High exposure images of immunoblots in B and C, respectively, to better visualize accumulation of truncated fragments Syn10 and Syn8 in P100. **F**, **G**, **H**, Quantitative analysis of relative density of αS truncated fragments in P10 and P100 respectively in PreS, sick Ctx or SpC, obtained by normalization with human αS full length monomer detected with LB509. Values are expressed as % of P10 and are given as the mean ± SD (n = 3 or 4). *p < 0.05, **p < 0.001, Student's t-test.

specific accumulation of phosphorylated HMW bands. Analysis of Ctx of diseased mice showed a slight increase in oligomers/aggregates and phosphorylated αS in P100, with respect to P10, although much less abundant than in affected SpC, suggesting that early signs of αS aggregation appear initially in the P100/M fraction.

Taken together these results suggest that specific features such as increased aggregation, truncation and phosphorylation can define a distinctive specie of αS associated with the P100/M vesicles.

### 3.2. Spreading of αS aggregate fractions in mouse primary hippocampal and cortical neurons

In order to understand whether αS species present in P10 and P100 fractions induce toxicity to neurons, we added P10 and P100 fractions isolated from presymptomatic (SpC) and diseased mice (SpC or Ctx) in the conditioned medium of hippocampal or cortical primary neurons obtained from WT mice. To avoid sample variability, P10 or P100 were obtained by pooling fractions purified from 3 to 4 age-matched mice of the same condition.

Application of 1 μg of P100 fraction from sick mice to neuronal cultures resulted in the appearance of long strings of beads-like structures after two weeks of treatment, that were positive for αS aggregates specific antibodies such as pSer129-αS [Fig. 2 A, E(c)] and syn303 [Fig. 2 D, E (a,b)] and organized in a neurite-like pattern. Partial co-localization with neuronal synaptic and axonal markers such as mouse αS and Tau confirmed that these structures made of αS aggregates were indeed associated with the neurites network (Fig. 2C). Occasionally these strings appeared to co-localize and stain the cell soma or cover the

entire process, resembling necrotic neurites. In this latter case when cultures where stained with the neuronal marker syn1, the neurites network appeared to be less dense and more scattered when treated with P100 from sick mice, especially for cortical cultures, suggesting that the formation of these strings of αS aggregates might be detrimental for cells. While for P100 those structures were more abundant and covered the neuronal network extensively, administration of the same amount of P10 produced very few small and scattered strings that were more immature in size and number (Fig. 2). No major differences were detected in the formation of these strings of aggregates between hippocampal and cortical neurons (Fig. 2D). Further administration of P10 and P100 from presymptomatic mice or P100 from Ctx of sick mice or nTg littermates failed to produce any string-like structure positive for syn303 (Supplemental Fig. 2) or pSer129-αS (data not shown).

Formation of αS positive strings were also dose- and time-dependent since reducing by half (0.5 μg) the original dose of P100 fraction from SpC of sick mice or fixing neuronal cultures at earlier time points resulted in few scattered fibrillary structures or numerous premature puncta that while their amount increased over time, failed to form an elongated and complete string (Supplemental Fig. 3A,C) when analyzed at early time points. In both cases administration of P10 from sick mice failed to produce comparable string-like structures positive for syn303 or pSer129-αS.

To understand whether these strings of αS aggregates accumulated endogenously or were externally attached to the plasma membrane we used a protocol of "two-stage" immunofluorescence where labeling of P100-associated aggregates with pSer129-αS antibody was done in living neurons, before fixation and permeabilization. In this case the
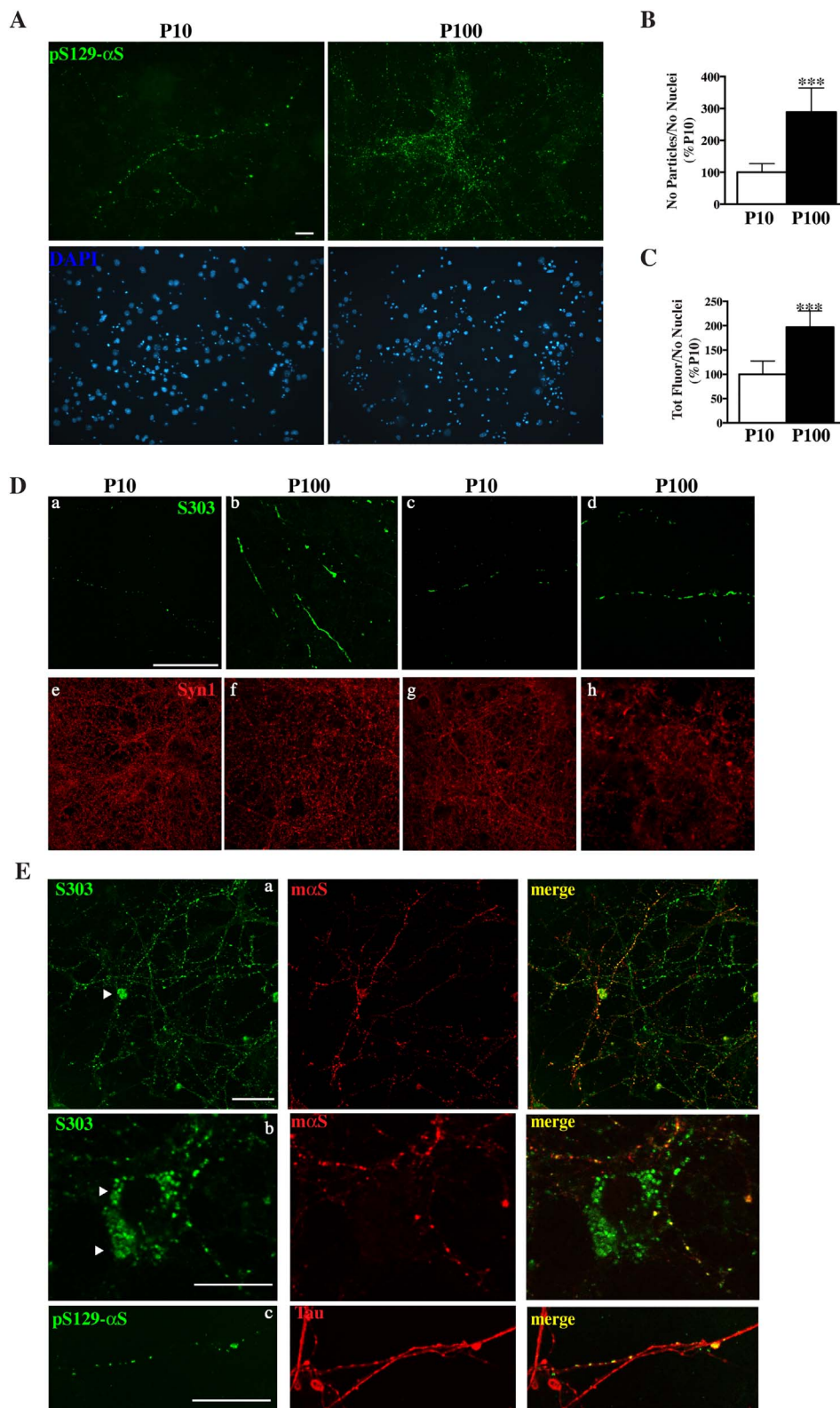
**A**



**B**



**C**



**D**



**E**



**Fig. 2.** Treatment with P100 fractions induced deposition of beads-like structures made of αS aggregates in primary murine neurons.

Formation of beads-like structures made of αS aggregates after administration of 1 μg of P10 or P100 fractions pooled from 3 to 4 SpC of sick mice to hippocampal [A, B (a,b)], or cortical primary neuronal cultures [B (c,d), C]. Cultures were fixed after 2 weeks of treatment and stained with pSer129-αS or Syn303 antibodies. **A**, Representative immunofluorescence images showing αS-positive strings after P10 and P100 treatment in hippocampal cultures stained with the pSer129-αS antibody. P100 administration induced deposition of beads-like structures organized in a string and following a neurite-like pattern. These strings were positive for αS aggregates specific antibodies such as pSer129-αS. Compared to P100, P10 treatment induced the formation of small puncta that resembled those obtained for P100 but were less abundant and more immature in size and number. Images were taken with Nikon Eclipse E600 epifluorescence microscope using a 20 × objective. Scale bar = 100 μm. **B, C**, Quantitative analysis of images in A showing increased accumulation of pSer129-αS positive structures in P100 treated cultures. Fluorescence signal was measured as total fluorescence after background subtraction (B) or as particles count (C) using Image J software. Both parameters were normalized with the total nuclei count (labeled with DAPI) per field. Values are expressed as % of P10 and are given as the mean ± SD ($n = 6$). ***$p < 0.0001$, Student's $t$-test. **D**, Confocal images showing that no major difference between hippocampal (a,b) or cortical (c,d) cultures were detected in the formation of αS-positive strings after administration of P10 or P100 obtained from SpC of sick mice. Occasionally αS strings after P100 treatment appear to cover the entire process, resembling necrotic neurites (b, d). To check the neuronal viability, cultures were also stained with syn1 antibody (red). Stacked images were acquired with a Leica confocal microscope SP2 system using a 63 × objective. Scale bar = 50 μm. **E**, Confocal images showing partial co-localization with neuronal markers such as mouse αS (mαS) (a,b) and Tau (c) in cortical primary cultures treated with P100 fractions from SpC of diseased mice. Occasionally these strings positive for αS aggregates co-localize and stain the cell soma (a and b arrow heads). Stacked images were acquired using a 63 × objective. Scale bar = 50 μm (a), 20 μm (b,c).

plasma membrane remains intact so only αS species that are not internalized by the neurons can be labeled. After incubation with the pSer129-αS antibody, cultures were extensively washed and then fixed, permeabilized and stained with the syn303 antibody in order to label all the aggregates, inside and outside the cell membrane. Surprisingly, all the P100 aggregates were labeled only with syn303 but not with pSer129-αS, indicating that P100-associated αS species are contained

within the neurons and not merely externally attached to the cell membrane (Fig. 3b). The lack of merged signal between syn303 and pSer129-αS also suggested that an active transport in living cells of membrane-bound antibodies was not significant in our conditions. Switching the antibody used in live neurons, *i.e.* incubating live primary cultures with syn303 and then staining with pSer129-αS antibody, did not affect the outcome of the two-stage immunofluorescence

experiment, since no syn303 staining was detected without permeabilization (Supplemental Fig. 4A). However, when neurons were fixed before the incubation with pSer129-αS and syn303, αS strings were mostly co-labeled by both antibodies, especially in the case of larger puncta, ruling out the possibility that competition for the same target could interfere with the aggregates staining by both antibodies at the same time. To confirm that αS aggregates that are externally associated with the cell membrane can be efficiently labeled following the "two-stage" immunofluorescence protocol we repeated this assay using neuroblastoma cell lines (SH-SY5Y) stably expressing WT αS tagged with Myc. When the P100 fraction was given to these cells and "two stage" immunofluorescence was performed, most of the aggregates were double labeled with pSer129-αS and syn303 antibodies, showing that most of the aggregates were found associated outside the cell membrane. Additionally, incubation of live neuronal cultures treated with buffer (B) with Map2 (Fig. 3a) or grp94 antibodies and SH-αS-Myc WT cells treated with grp94, according to the "two-stage" immuno-fluorescence protocol (Supplemental Fig. 4B) did not result in any staining unless cells were previously fixed, confirming that no antibodies can label cellular endogenous targets without previous fixation and permeabilization of the cellular membrane as done in our experimental settings. Moreover since the endosomal-lysosomal pathway has been implicated in the internalization of exogenous *in vitro* preformed αS fibrils (Karpowicz et al., 2017), double staining with syn303 and Lamp1, a lysosomal marker, was done in cortical neuronal culture after 2 days or 1 week of treatment with P100 fractions from SpC of sick Tg mice. We found little co-localization between syn303 and Lamp1 at both times, suggesting that the endosomal pathway might not be the preferential route of entry of P100-associated aggregates in primary neurons (Supplemental Fig. 5).

In summary, treatment with P100 fractions from diseased mice that contain microsomal-associated αS species induced the formation of string-like structures, positive for αS aggregates specific antibodies, that followed a neurite pattern and co-localized with synaptic and axonal markers.

### 3.3. Induction of apoptosis in mouse hippocampal and cortical primary culture treated with P100 from SpC of presymptomatic and diseased mice

Increasing the concentration of the above fractions to 2 μg resulted in induction of apoptosis only in primary cultures treated with P100 fractions obtained from SpC of diseased mice and more surprisingly from presymptomatic littermates, as shown by the increase in TUNEL staining and the concomitant decrease of neuronal survival measured by NeuN labeling (Fig. 4). No neuronal degeneration in cultures treated with P10 from sick and presymptomatic mice, P100 Ctx or P100 nTg was observed. Although TUNEL levels were comparable between presymptomatic and sick P100 fractions, the NeuN-positive count was actually higher in presymptomatic P100-treated samples, suggesting that αS species associated with microsomal fractions obtained from healthy aged animals were less aggressive in inducing cellular death. In the first experiments, although early signs of cellular death were visible
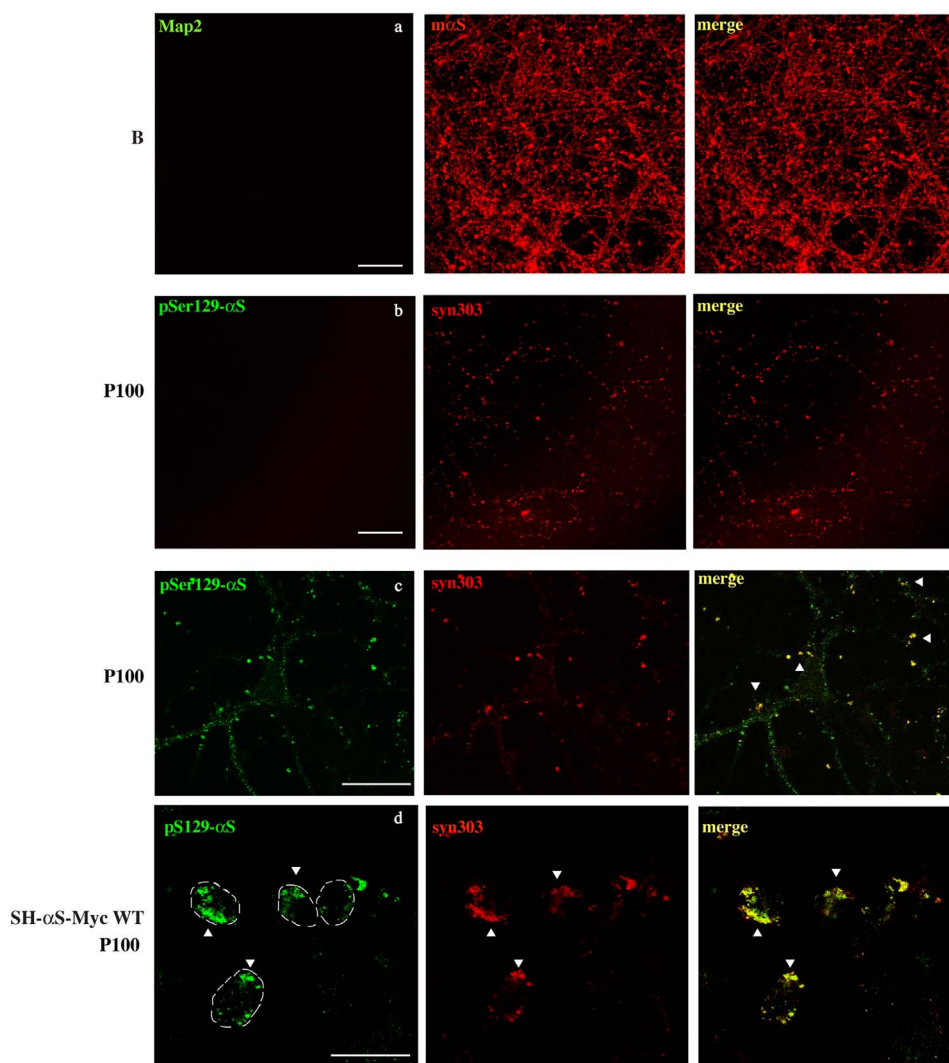


**Fig. 3.** Internalization and spreading of P100 fractions into neuronal cultures.

Two-stage immunofluorescence showed how αS aggregates spread into within the neurons to form αS positive strings. Live hippocampal neurons treated with buffer (B) (a), P100 fractions from sick SpC (b) or SH-SY5Y neuroblastoma cells stable for αS expression (SH-αS-Myc WT) treated with 5 μg of P100 sick SpC (d) were incubated at 4 °C with Map2 or pSer129-αS antibody, for 30 min before being fixed, permeabilized and stained with mαS or syn303 antibody, respectively. Confocal stacked images were acquired with a 63 × objective. Absence of merged signals showed that no antibodies can label endogenous target without previous fixing and permeabilization of the cell membrane indicating that most of the αS aggregates are internalized by neurons. When neurons treated with P100 sick SpC were instead fixed (c) before pSer129-αS and syn303 incubation, both antibodies label αS strings (arrow heads), although not with the same efficiency. On the contrary, merged signals between pSer129-αS and syn303 in SH-αS-Myc WT treated with P100 pellet from Sick SpC (d, arrow heads) demonstrated that αS aggregates are not internalized in this cell model. Thus only in the case of αS aggregates externally attached to the neurite membrane or the cell membrane being permeabilized, both antibodies can co-label αS aggregates. In d) a white line showing the cell borders was drawn by overlapping fluorescence with regular white light images taken at the same time. Scale bar = 50 μm (a,b,c), 20 μm (d).

as soon as 24–48 hrs after addition, neurons were fixed after 3 days of treatment when neuronal degeneration in P100 sick treated cultures became widespread. When we let the treatment go further and fixed cultures after a week, cell death was so exhausted in P100 sick-treated neurons that very few cells (DAPI-positive nuclei) were left in the well. In this case also neurons treated with P100 from presymptomatic mice showed remarkable levels of cell death and neuronal loss, comparable to what has been observed previously in cultures treated with P100 sick and fixed after 3 days (Supplemental Fig. 6). At the same time also cultures treated with P10 from sick animals started to show a slight decrease in NeuN-positive neuronal count and an increased in TUNEL staining, showing that P10-associated αS aggregates can also be toxic but not as aggressive as the P100 counterpart in inducing neuronal death. Although TUNEL levels in sick P10-treated neurons were

comparable with the amount of cell death in cultures treated with presymptomatic P100, the decrease in neuronal loss was not as remarkable, suggesting that neuronal degeneration was delayed compared to PreS-P100 treated cultures. Interestingly P10 from presymptomatic mice was never able to induce apoptosis in primary cultures in our experimental setting, while a mild decrease in neurons viability was observed for P100 Ctx-treated cultures, although was not significant, for prolonged treatment. Thus, only microsomal fractions obtained from diseased or presymptomatic affected areas have an enhanced ability to induce cellular death in primary neuronal cultures therefore are more toxic than P10. Interestingly, the only feature that the P100 from presymptomatic and diseased areas have in common in terms of αS structural or posttranslational modifications is the presence of αS oligomers, suggesting that other modifications such as
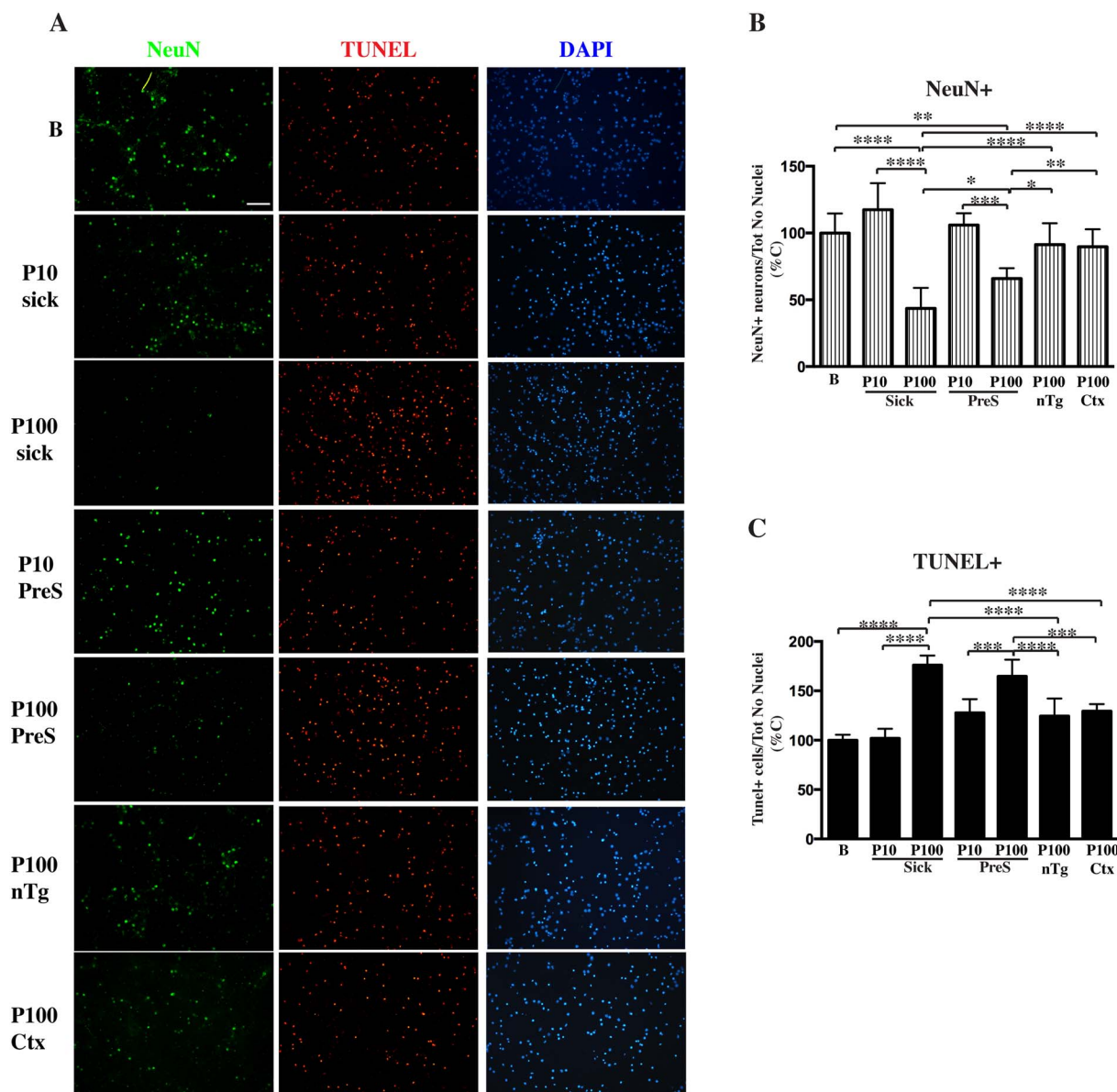


Fig. 4. Induction of neuronal death in primary neurons after treatment with P10 and P100.
Primary hippocampal neurons were treated with 2 μg of various P10 and P100 pellet obtained from presymptomatic or diseased SpC and Ctx of Tg mice and age-matched Ntg littermates or buffer (B). Cultures were fixed after 3 days of treatment and co-labeled with NeuN and Tunel staining. Cultures were also counterstained with Dapi. **A**, Representative fluorescent images showing induction of apoptosis and concomitant decrease in neurons viability only in primary cultures treated with P100 fractions obtained from SpC of diseased mice and more surprisingly from presymptomatic littermates. Fluorescent images were acquired with a Nikon epi-fluorescence microscope using a 20 × objective and cell counting was done using Image J software. Scale bar = 100 μm. **B, C**, Quantitative analysis of images in the panel A for live NeuN-positive neurons (B) or dead Tunel-positive neurons (C). Live or dead cell counts were normalized for the number of Dapi-positive nuclei. Values are expressed as % of control neurons treated with buffer and are given as the mean ± SD ($n = 6$). *$p < 0.05$, **$p < 0.001$, ***$p < 0.0001$, ****$p < 0.00001$, one-way ANOVA, followed by Tukey post-hoc test.
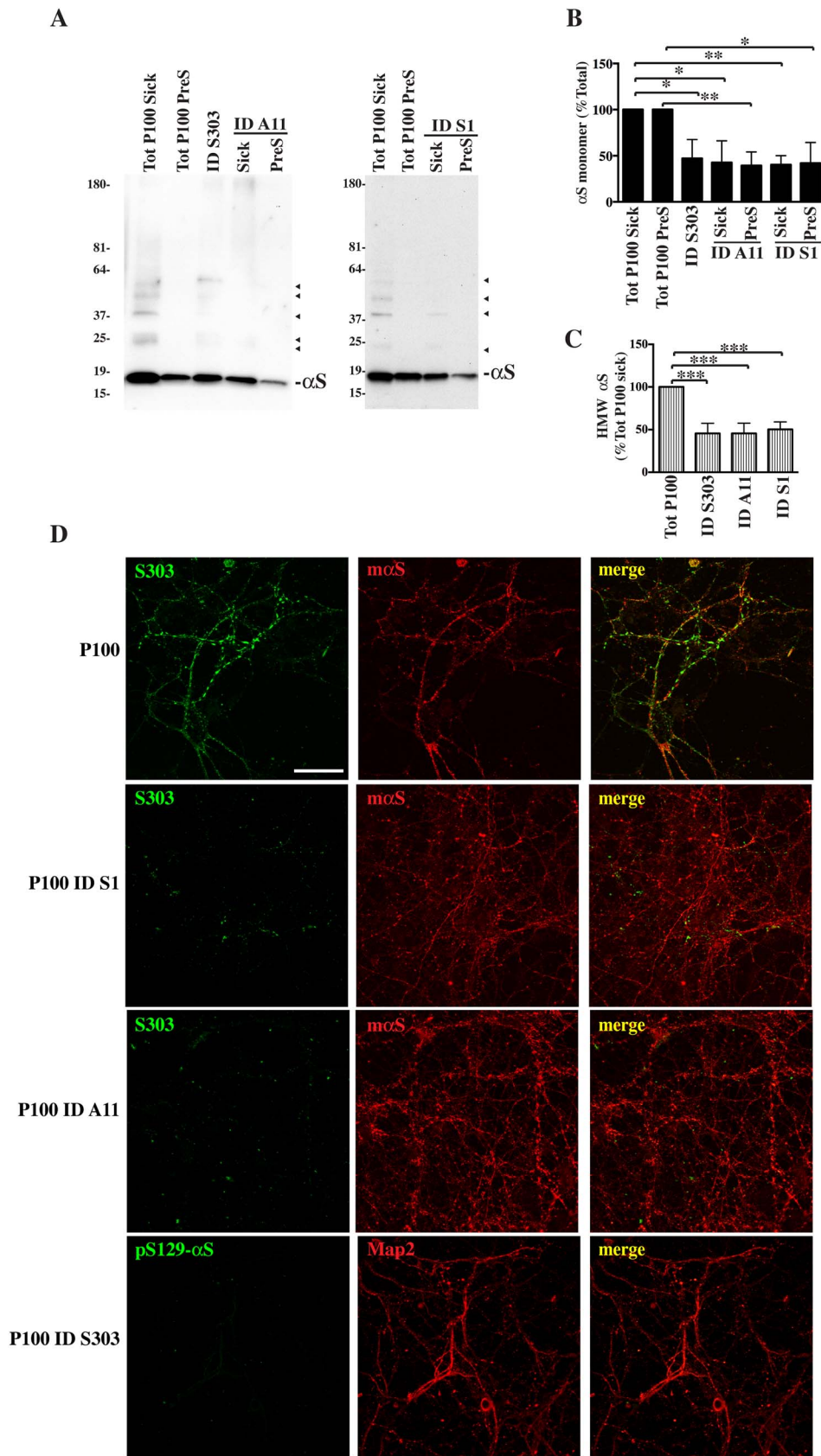
**A**



**B**



**C**



**D**



**Fig. 5.** Immunodepletion of αS toxic species from P100 prevents formation of αS strings.

To check if αS species associated with microsomes were indeed responsible for cellular modifications described above we perform immunodepletion of αS species from the P100 fractions by incubating P100 with protein agarose conjugated with Syn1 (S1), Syn303 (S303) or A11. **A**, Shows immunoblotting of P100 immune-depleted (ID) fractions run along total P100 pellets from presymptomatic (Tot P100 PreS) or diseased mice (Tot P100 Sick). Samples were transferred to a nitrocellulose membrane and blotted with Syn1 antibody. **B, C**, Quantitative analysis of αS full length monomer (B) or HMW species (C) as shown in A indicates a reduction in αS content for all species after immunodepletion in P100 ID fractions. Densitometric analysis of HMW bands was done by measuring the relative intensity for the whole sample lane above the monomer. Values are expressed as % of corresponding total P100 pools, sick or presymptomatic, and given as the mean ± SD ($n = 3$). *$p < 0.05$, **$p < 0.001$ One-way ANOVA, followed by Tukey post-hoc test. **C**, 1 μg of ID and original P100 samples from diseased were given to hippocampal neurons. Cells were fixed and immunostained with syn303/mαS or pSer129-αS/Map2 after 2 weeks. Stacked fluorescent images taken at the confocal microscope showed a drastic decrease in the formation of αS aggregates-positive strings. Scale bar = 50 μm.

phosphorylation and truncation are not necessary for αS acquired toxicity.

### 3.4. Partial depletion of the αS species from P100 fractions from diseased and presymptomatic mice prevents spreading and induced toxicity in primary cultures

To establish whether αS species contained in P100 fractions were indeed responsible for the induction of apoptosis, immunodepletion with various αS antibodies that recognize specific αS conformations (A11 for αS oligomers, syn303 for αS aggregates and Syn1 for total αS) was performed from pooled P100 fractions from SpC of diseased and presymptomatic mice. Briefly, P100 fractions were incubated with the above antibodies, previously conjugated with protein-binding agarose, for 1 hr at 4 °C. After spinning at low speed the supernatant was carefully recovered and checked for the content of αS species. αS monomer and HMW species levels in immunodepleted (ID) samples were dramatically reduced to about 40–45% or 45–50%, respectively, of the original total pools amount (Fig. 5 A, B, C). ID samples were then dosed to cortical neuronal cultures and formation of αS strings and neuronal death was evaluated. While neurons treated with P100 obtained from SpC of sick mice developed αS aggregates-positive strings, cultures treated with ID sick samples did not. More specifically, neurons treated with ID Syn1 sick or ID A11 sick fractions showed scattered dot-like αS structures not yet organized in a string pattern, more abundant in ID A11 than ID Syn1, while ID syn303 sick-treated cultures showed only very few small puncta positive for αS (Fig. 5C).

When we checked for toxicity, in the case of neurons treated with P100 pooled from SpC of sick mice, cell death was already apparent after 24–48 hrs of treatment. Nevertheless, to see if αS depletion could effectively rescue neurons, cultures were not fixed immediately but the treatment was continued to make sure that any possible rescuing effect that we would see was not due to a time frame difference. When cultures were then analyzed for cell survival, neuronal degeneration in P100 sick-treated cultures was exhaustive. In fact, the number of NeuN-positive neurons (Fig. 6) had dramatically dropped only in samples treated with P100 sick fractions but not in cultures treated with ID sick fractions, suggesting that depletion of αS helped keep neurons healthy. Interestingly immunodepletion of mature αS aggregates with syn303 was more efficient in preventing αS-induced toxicity than the abrogation of total αS in ID Syn1 samples, suggesting that toxicity is due to the presence of αS HMW conformers rather than αS itself after disease onset. Moreover while treatment with ID Syn1 and A11 seemed to only delay cell death as shown by increased Tunel positivity compared to P100 and control samples (Fig. 6C), immunodepletion with syn303 constitutively blocked apoptosis reducing Tunel level lower than untreated samples.

In the case of presymptomatic fractions, the number of NeuN-positive neurons was significantly reduced only in cultures treated with P100 PreS, but not in P100 PreS ID treated samples. Here immunodepletion with Syn 1 or A11 fully rescued neuronal cultures and blocked cellular death as shown by reduced Tunel levels.

Thus reduced spreading of αS aggregates due to immunodepletion prevents neuronal degeneration in murine primary neurons, indicating that αS species contained in P100 pools are responsible for neurodegeneration after administration to primary neuronal cultures.

### 4. Discussion

The results presented here indicate that within the heterogeneity of αS HMW species there is a small, unique fraction that is more aggressive in terms of propagation and toxicity. This population of extremely toxic αS species is associated with the microsomal vesicles and presents specific biochemical traits such as increased aggregation, truncation and phosphorylation at serine 129 that makes them unique.

The hypothesis of an extremely detrimental factor or species within

the αS HMW population has been long postulated (Caughey and Lansbury, 2003) and not only in PD but in other neurodegenerative diseases as well (Ugalde et al., 2016). Initially questions arose regarding the potential toxicity of αS oligomers as opposed to mature fibrils to explain, for example, early observations on why dopaminergic neurons bearing LBs appeared to be healthier than neighboring neurons (Tompkins and Hill, 1997). Since then a significant body of evidence, describing αS different oligomer conformations *in vitro* and their associated mechanism of toxicity has been generated (Roberts and Brown, 2015), despite that the *in vivo* presence of αS oligomers has been controversial and particularly difficult to characterize (Colla et al., 2012b). On the opposite, more recent data (Luk et al., 2009, 2012; Volpicelli-Daley et al., 2011) including an investigation led by V. Baekelandt showed that both *in vitro* pre-formed oligomers and fibrils are indeed neurotoxic but display different seeding capacity and induce different histopathological and behavioral abnormalities when injected in rats (Peelaerts et al., 2015). Thus it appears that structure does not necessarily dictate toxicity, or at least in part, since both αS oligomers and fibrils seems to contribute to neuronal degeneration.

While most of the evidence accumulated until now to prove the enhanced capacity of oligomers or aggregates to induce toxicity focused on structural differences, in this paper, we took a different approach and we focused our attention on the different subcellular location of αS HMW species rather than their conformation.

By isolating αS HMW species from a Tg mouse model for αS expression, and separating them according to their molecular weight and/or membrane-association, we showed how the ER/M-associated αS pool is remarkably neurotoxic and able to seed formation of αS-positive strings in primary neurons when compared to the rest of αS HMW species that precipitates at low speed (P10). αS association and localization within the ER/M system in normal and diseased conditions has been demonstrated in cultured cells, in neurons of Tg mice and PD brain by biochemical isolation, cell imaging and electron microscopy (Colla et al., 2012a, 2012b; H.-J. Lee et al., 2002; Lee et al., 2005). Given the presynaptic localization of αS, its ability to bind to synaptic vesicles through the SNARE complex and to inhibit the ER-Golgi transport (Burre et al., 2010; Burré et al., 2014; Cooper et al., 2006; Thayanidhi et al., 2010), it is not surprising to find a weak association of αS with microsomal vesicles, which is a raw pellet fraction containing ER, Golgi e synaptic vesicles, in normal conditions (Colla et al., 2012a). Instead, with αS aggregation and disease onset, the partitioning between membranous-bound and free αS changes and there is an increased redistribution of αS to P100/M membranes (Colla et al., 2012a). This could be due to an increase of αS protein stability and reduced turnover correlated to change in conformation and protein solubility or to an increased sequestration of free αS by aggregates. Interestingly, at the presynaptic level, others have shown how free presynaptic αS can be recruited into insoluble aggregates (Volpicelli-Daley et al., 2011) and how presynaptic αS small aggregates might be more detrimental than LB and correlate better with synapses dysfunction *in vivo* (Kramer and Schulz-Schaeffer, 2007).

Association with the microsomal membrane seems to be very specific since although P10 contains membranous components that include the mitochondria and MAM, we never found αS HMW species co-precipitating with this organelle when we purified mitochondria from affected areas in the same mouse model (Colla et al., 2012b). In contrast, we found a strong association between αS aggregates and the ER membrane as shown by the ability of αS aggregates to float and partition with the membranous component on a lipid flotation assay when isolated as a P100/Microsomal pellet. Very interestingly when the membranous component of P100 was removed by the addition of non-ionic detergent and the lipid flotation analysis was repeated, ER-associated αS aggregates did not partition with the membrane fraction, demonstrating that αS aggregates actively bind the ER/Microsomal membrane (Colla et al., 2012a). In addition accumulation of αS pathological changes such as formation of αS aggregates, truncation and
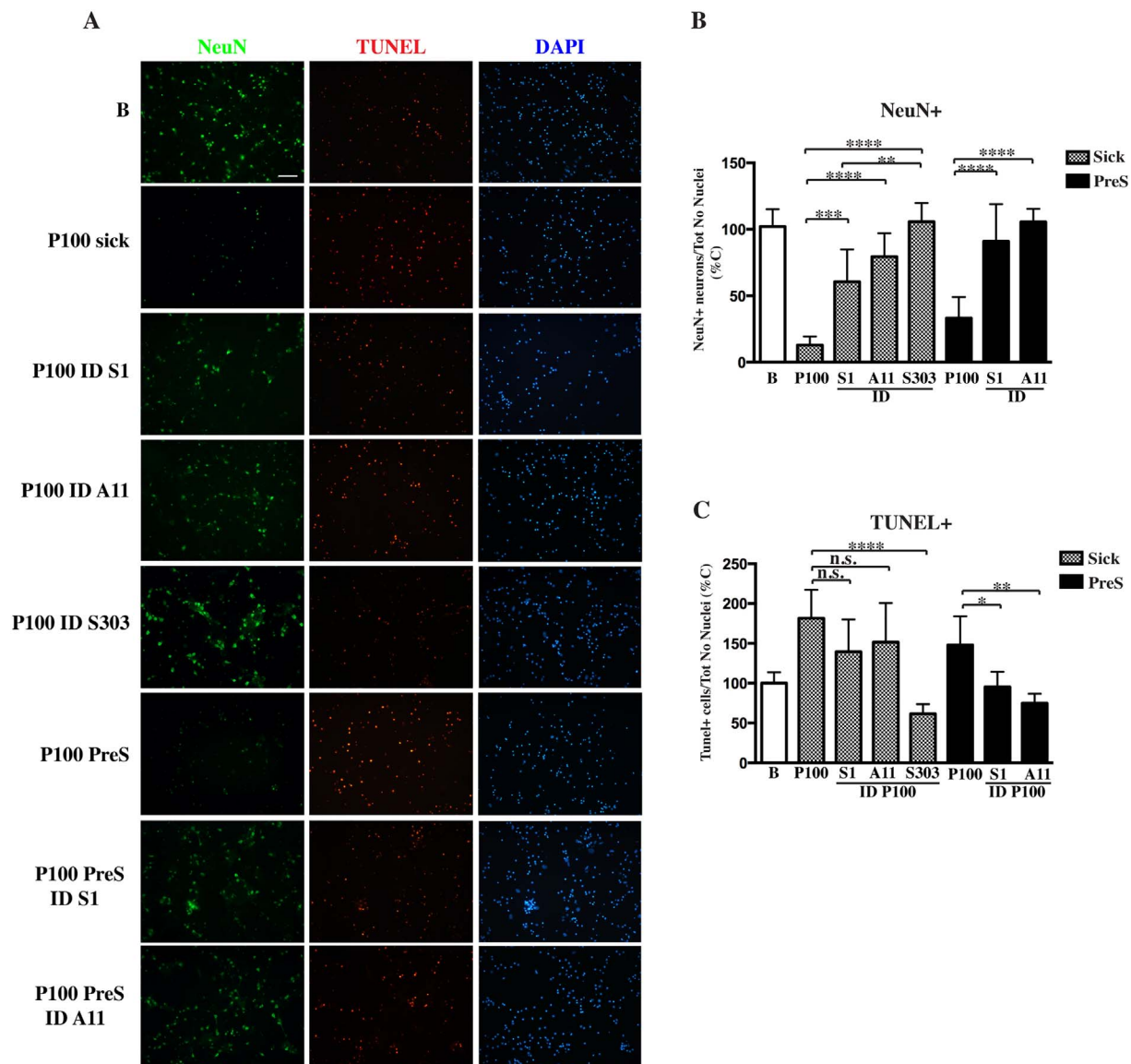
**Fig. 6.** Immunodepletion of αS toxic species from P100 prevents neurodegeneration in murine primary cultures.

2 µg of ID and total P100 samples from diseased and presymptomatic mice or buffer (B) were administered to hippocampal neurons in culture. **A**, Representative images of immunostaining with NeuN antibody or Tunel shows an increase in cell survival and concomitant reduction in neuronal death in cultures treated with ID samples obtained from presymptomatic and sick mice. Fluorescent images were acquired with a Nikon epi-fluorescence microscope using a 20 × objective. Scale bar = 100 µm. **B, C**, Cell survival graph of NeuN-positive neurons (B) or Tunel staining (C) after administration of ID and total fractions showed how reduction in P100-associated αS toxic species prevents cell death. Values were normalized for the number Dapi-positive nuclei and expressed as % of neurons treated with buffer. In the graph each column represents the mean ± SD ($n = 6$). *$p < 0.05$, **$p < 0.001$, ***$p < 0.0001$, ****$p < 0.00001$, One-way ANOVA, followed by Tukey post-hoc test.

phosphorylation are more likely to occur close to the ER/M membranes. Similarly because of this association it is also plausible that in patho-physiological conditions the first changes implicated in αS acquired toxicity occur at the ER/M membranes level. Thus association with the microsomal membranes seems to be a key step for αS acquired toxicity.

Although it remains unclear what is the pathological role of all the changes associated with neurotoxicity that αS undergoes, the cortical region in Prp A53T mice may be a good model to study early changes in αS toxic modifications. In fact, although the cortical regions in Prp A53T mice have no overt accumulation of αS aggregates and LB-like inclusions, nor neuronal degeneration or gliosis (M. K. Lee et al., 2002), the P100 fractions obtained from Ctx of sick mice did show mild early changes in protein truncation, phosphorylation or accumulation of αS oligomers/aggregates that may resemble an intermediate condition between presymptomatic and disease. At the same time P100 Ctx fraction did not significantly induce cell death when given to primary

cultures, indicating these initial changes in αS are not sufficient to induce an overt neuronal degeneration.

Once administered to primary neurons, P100/M-associated αS toxic species from diseased mice quickly spread into neurons in a similar manner to what has been described by V. Lee and coworkers (Volpicelli-Daley et al., 2011, 2014). In their work, *in vitro* assembled αS fibrils initially induced the deposition of strings of small puncta within neurites, resembling what we obtained when low amount of P100 Sick SpC was used or when neuronal cultures were fixed at early time points (Supplemental Fig. 3), which subsequently developed into fibrous structures covering processes and soma. Although we only occasionally saw accumulation of fibrous strings in the neuronal cell body, probably because of the difficulty in finely adjusting the titration of P10 and P100 fractions in our cultures, the fibrous structures described by Volpicelli-Daley's paper are comparable to what we obtained by treating neurons with increasing concentration of P100/M fractions

from Sick SpC. In addition the dose- and time-dependent formation of αS fibrous strings and their co-localization with mouse endogenous αS may suggest that mouse αS could become entangled and recruited into these bead-like structures, similarly to what have been previously described after administration of *in vitro* preformed αS fibrils (Volpicelli-Daley et al., 2011). However, since the co-localization with mouse αS was only partial, it is unlikely that the formation of αS strings in cultured neurons is only due to aggregated mouse αS. In the same way the limited co-localization between Tau and αS strings suggested a lower chance for Tau to cross-seeds αS aggregates deposition after P100 administration.

In terms of amount of cell toxicity of P100/M fractions from sick SpC was far more detrimental than what V. Lee's paper suggested (Volpicelli-Daley et al., 2011), considering that the dosage we used was lower and far less concentrated. Thus, a small amount of P100/M-associated αS was sufficient to induce a massive apoptotic response in primary neurons (Figs. 4, 6). Levels of cell death in neurons treated with P100 PreS were remarkably higher than with P10 Sick, indicating that before accumulation of αS oligomers/aggregates and aggregation-related modifications, some toxic αS species associated with the microsomal membrane were already present. Despite that, we were never able to observe deposition of any αS puncta or string in presymptomatic-treated cultures with aggregates-specific antibodies (syn303 or pSer129-αS) or with a human αS antibody, confirming that soluble toxic forms of αS have different seeding properties from fibrils (Peelaerts et al., 2015) and that αS oligomers do not need to become mature aggregates to be toxic. Also because of the toxicity of αS associated with P100 PreS, it appears that accumulation of truncated and/or phosphorylated species is only secondary and does not account for the acquired ability to induce neuronal death. Moreover, immunodepletion experiments showed how the toxic function of αS depends on its internalization and propagation rather than a mere activation of a cell death cascade from the cell membrane. In fact treatment with P100 ID samples prevented induction of neuronal death and a correspondent striking reduction in the formation of αS-positive neuritic strings (Figs. 5, 6). Thus our data point to a change in structure and a specific interaction with the ER/M, shown by the abundant presence of soluble αS oligomers in the P100/M fractions of diseased and presymptomatic mice (Supplemental Fig. 1 and (Colla et al., 2012b) as the main culprit of αS propagation and neuronal degeneration.

## 5. Conclusions

Our results have demonstrated the *in vivo* existence of a toxic pool of αS HMW species associated with the ER/M vesicles. Our data suggests that the first pathological changes in αS behavior appear in the small portion of αS associated with the microsomal vesicles, (probably at a presynaptic level). It is not yet clear whether other αS aggregates (that we concentrated in P10) derived from the microsomes-associated pool or form independently. While more studies will be necessary, our findings provide the first insights in the pathological behavior of αS *in vivo*, shining a critical spotlight on the association with the P100/M membranes as a necessary step toward the acquisition of αS toxicity.

Supplementary data to this article can be found online at https://doi.org/10.1016/j.nbd.2017.12.004.

## Acknowledgements

## Author contributions

EC, GP, AR, VV performed the experiments; EC designed the research, wrote the paper and analyzed the data; CR, LR and FG isolated murine primary neurons and helped with cell cultures; NC, SC provided technical assistance with mice husbandry; MKL provided the murine transgenic model and reviewed the manuscript; AC reviewed the manuscript. All authors read and approved the final manuscript.

## Competing interests

The authors declare that they have no competing interests.

## Ethics approval

All animal studies were approved and complied in full by the national and international laws for laboratory animal welfare and experimentation (EEC council directive 86/609, 12 December 1987 and Directive 2010/63/EU, 22 September 2010).

## References

Appel-Cresswell, S., Vilarino-Guell, C., Encarnacion, M., Sherman, H., Yu, I., Shah, B., Weir, D., Thompson, C., Szu-Tu, C., Trinh, J., Aasly, J.O., Rajput, A., Rajput, A.H., Jon Stoessl, A., Farrer, M.J., 2013. Alpha-synuclein p.H50Q, a novel pathogenic mutation for Parkinson's disease. Mov. Dis. Off. J. Mov. Dis. Soc. 28, 811–813. http://dx.doi.org/10.1002/mds.25421.

Bartels, T., Choi, J.G., Selkoe, D.J., 2011. α-Synuclein occurs physiologically as a helically folded tetramer that resists aggregation. Nature 477, 107–110. http://dx.doi.org/10.1038/nature10324.

Beaudoin, G.M.J., Lee, S.-H., Singh, D., Yuan, Y., Ng, Y.-G., Reichardt, L.F., Arikkath, J., 2012. Culturing pyramidal neurons from the early postnatal mouse hippocampus and cortex. Nat. Protoc. 7, 1741–1754. http://dx.doi.org/10.1038/nprot.2012.099.

Bendor, J.T., Logan, T.P., Edwards, R.H., 2013. The function of α-synuclein. Neuron 79, 1044–1066. http://dx.doi.org/10.1016/j.neuron.2013.09.004.

Burré, J., 2015. The synaptic function of α-synuclein. J. Parasit. Dis. 5, 699–713. http://dx.doi.org/10.3233/JPD-150642.

Burré, J., Sharma, M., Tsetsenis, T., Buchman, V., Etherton, M.R., Sudhof, T.C., 2010. α-Synuclein promotes SNARE-complex assembly in vivo and in vitro. Science 329, 1663–1667. http://dx.doi.org/10.1126/science.1195227.

Burré, J., Vivona, S., Diao, J., Sharma, M., Brunger, A.T., Südhof, T.C., 2013. Properties of native brain α-synuclein. Nature 498, E4-6-7. http://dx.doi.org/10.1038/nature12125.

Burré, J., Sharma, M., Südhof, T.C., 2014. α-Synuclein assembles into higher-order multimers upon membrane binding to promote SNARE complex formation. Proc. Natl. Acad. Sci. 111, E4274–E4283. http://dx.doi.org/10.1073/pnas.1416598111.

Caughey, B., Lansbury, P.T., 2003. Protofibrils, pores, fibrils, and neurodegeneration: separating the responsible protein aggregates from the innocent bystanders. Annu. Rev. Neurosci. 26, 267–298. http://dx.doi.org/10.1146/annurev.neuro.26.010302.081142.

Chandra, S., Chen, X., Rizo, J., Jahn, R., Südhof, T.C., 2003. A broken alpha-helix in folded alpha-synuclein. J. Biol. Chem. 278, 15313–15318. http://dx.doi.org/10.1074/jbc.M213128200.

Chartier-Harlin, M.-C., Kachergus, J., Roumier, C., Mouroux, V., Douay, X., Lincoln, S., Levecque, C., Larvor, L., Andrieux, J., Hulihan, M., Waucquier, N., Defebvre, L., Amouyel, P., Farrer, M., Destée, A., 2004. α-Synuclein locus duplication as a cause of familial Parkinson's disease. Lancet 364, 1167–1169. http://dx.doi.org/10.1016/S0140-6736(04)17103-1.

Colla, E., Coune, P., Liu, Y., Pletnikova, O., Troncoso, J.C., Iwatsubo, T., Schneider, B.L., Lee, M.K., 2012a. Endoplasmic reticulum stress is important for the manifestations of α-synucleinopathy in vivo. J. Neurosci. 32, 3306–3320. http://dx.doi.org/10.1523/JNEUROSCI.5367-11.2012.

Colla, E., Jensen, P.H., Pletnikova, O., Troncoso, J.C., Glabe, C., Lee, M.K., 2012b. Accumulation of toxic-synuclein oligomer within endoplasmic reticulum occurs in α-synucleinopathy in vivo. J. Neurosci. 32, 3301–3305. http://dx.doi.org/10.1523/JNEUROSCI.5368-11.2012.

Conway, K.A., Harper, J.D., Lansbury, P.T., 1998. Accelerated in vitro fibril formation by a mutant alpha-synuclein linked to early-onset Parkinson disease. Nat. Med. 4, 1318–1320. http://dx.doi.org/10.1038/3311.

Cooper, A.A., Gitler, A.D., Cashikar, A., Haynes, C.M., Hill, K.J., Bhullar, B., Liu, K., Xu,

K., Strathearn, K.E., Liu, F., Cao, S., Caldwell, K.A., Caldwell, G.A., Marsischky, G., Kolodner, R.D., Labaer, J., Rochet, J.-C., Bonini, N.M., Lindquist, S., 2006. Alpha-synuclein blocks ER-Golgi traffic and Rab1 rescues neuron loss in Parkinson's models. Science 313, 324–328. http://dx.doi.org/10.1126/science.1129462.

Cremades, N., Cohen, S.I.A., Deas, E., Abramov, A.Y., Chen, A.Y., Orte, A., Sandal, M., Clarke, R.W., Dunne, P., Aprile, F.A., Bertoncini, C.W., Wood, N.W., Knowles, T.P.J., Dobson, C.M., Klenerman, D., 2012. Direct observation of the interconversion of normal and toxic forms of α-synuclein. Cell 149, 1048–1059. http://dx.doi.org/10.1016/j.cell.2012.03.037.

Deleersnijder, A., Gerard, M., Debyser, Z., Baekelandt, V., 2013. The remarkable conformational plasticity of alpha-synuclein: blessing or curse? Trends Mol. Med. 19, 368–377. http://dx.doi.org/10.1016/j.molmed.2013.04.002.

Dettmer, U., Newman, A.J., Soldner, F., Luth, E.S., Kim, N.C., von Saucken, V.E., Sanderson, J.B., Jaenisch, R., Bartels, T., Selkoe, D., 2015. Parkinson-causing α-synuclein missense mutations shift native tetramers to monomers as a mechanism for disease initiation. Nat. Commun. 6, 7314. http://dx.doi.org/10.1038/ncomms8314.

Fauvet, B., Mbefo, M.K., Fares, M.-B., Desobry, C., Michael, S., Ardah, M.T., Tsika, E., Coune, P., Prudent, M., Lion, N., Eliezer, D., Moore, D.J., Schneider, B., Aebischer, P., El-Agnaf, O.M., Masliah, E., Lashuel, H.A., 2012. α-Synuclein in central nervous system and from erythrocytes, mammalian cells, and *Escherichia coli* exists predominantly as disordered monomer. J. Biol. Chem. 287, 15345–15364. http://dx.doi.org/10.1074/jbc.M111.318949.

Goedert, M., Spillantini, M.G., Del Tredici, K., Braak, H., 2012. 100 years of Lewy pathology. Nat. Rev. Neurol. 9, 13–24. http://dx.doi.org/10.1038/nrneurol.2012.242.

Golovko, M.Y., Faergeman, N.J., Cole, N.B., Castagnet, P.I., Nussbaum, R.L., Murphy, E.J., 2005. Alpha-synuclein gene deletion decreases brain palmitate uptake and alters the palmitate metabolism in the absence of alpha-synuclein palmitate binding. Biochemistry (Mosc) 44, 8251–8259. http://dx.doi.org/10.1021/bi0502137.

Golovko, M.Y., Barceló-Coblijn, G., Castagnet, P.I., Austin, S., Combs, C.K., Murphy, E.J., 2009. The role of α-synuclein in brain lipid metabolism: a downstream impact on brain inflammatory response. Mol. Cell. Biochem. 326, 55–66. http://dx.doi.org/10.1007/s11010-008-0008-y.

Iwai, A., Masliah, E., Yoshimoto, M., Ge, N., Flanagan, L., Rohan de Silva, H., Kittel, A., Saitoh, T., 1995. The precursor protein of non-Aβ component of Alzheimer's disease amyloid is a presynaptic protein of the central nervous system. Neuron 14, 467–475. http://dx.doi.org/10.1016/0896-6273(95)90302-X.

Karpowicz, R.J., Haney, C.M., Mihaila, T.S., Sandler, R.M., Petersson, E.J., Lee, V.M.-Y., 2017. Selective imaging of internalized proteopathic α-synuclein seeds in primary neurons reveals mechanistic insight into transmission of synucleinopathies. J. Biol. Chem. 292, 13482–13497. http://dx.doi.org/10.1074/jbc.M117.780296.

Kramer, M.L., Schulz-Schaeffer, W.J., 2007. Presynaptic-synuclein aggregates, not Lewy bodies, cause neurodegeneration in dementia with Lewy bodies. J. Neurosci. 27, 1405–1410. http://dx.doi.org/10.1523/JNEUROSCI.4564-06.2007.

Krüger, R., Kuhn, W., Müller, T., Woitalla, D., Graeber, M., Kösel, S., Przuntek, H., Epplen, J.T., Schöls, L., Riess, O., 1998. Ala30Pro mutation in the gene encoding alpha-synuclein in Parkinson's disease. Nat. Genet. 18, 106–108. http://dx.doi.org/10.1038/ng0298-106.

Lee, H.-J., Choi, C., Lee, S.-J., 2002. Membrane-bound-synuclein has a high aggregation propensity and the ability to seed the aggregation of the cytosolic form. J. Biol. Chem. 277, 671–678. http://dx.doi.org/10.1074/jbc.M107045200.

Lee, M.K., Stirling, W., Xu, Y., Xu, X., Qui, D., Mandir, A.S., Dawson, T.M., Copeland, N.G., Jenkins, N.A., Price, D.L., 2002. Human alpha-synuclein-harboring familial Parkinson's disease-linked Ala-53 → Thr mutation causes neurodegenerative disease with alpha-synuclein aggregation in transgenic mice. Proc. Natl. Acad. Sci. U. S. A. 99, 8968–8973. http://dx.doi.org/10.1073/pnas.132197599.

Lee, H.-J., Patel, S., Lee, S.-J., 2005. Intravesicular localization and exocytosis of alpha-synuclein and its aggregates. J. Neurosci. 25, 6016–6024. http://dx.doi.org/10.1523/JNEUROSCI.0692-05.2005.

Lesage, S., Anheim, M., Letournel, F., Bousset, L., Honoré, A., Rozas, N., Pieri, L., Madiona, K., Dürr, A., Melki, R., Verny, C., Brice, A., for the French Parkinson's Disease Genetics Study Group, 2013. G51D α-synuclein mutation causes a novel Parkinsonian-pyramidal syndrome: SNCA G51D in Parkinsonism. Ann. Neurol. 73, 459–471. http://dx.doi.org/10.1002/ana.23894.

Li, W., 2004. Stabilization of -synuclein protein with aging and familial Parkinson's disease-linked A53T mutation. J. Neurosci. 24, 7400–7409. http://dx.doi.org/10.1523/JNEUROSCI.1370-04.2004.

Li, W., West, N., Colla, E., Pletnikova, O., Troncoso, J.C., Marsh, L., Dawson, T.M., Jäkälä, P., Hartmann, T., Price, D.L., Lee, M.K., 2005. Aggregation promoting C-terminal truncation of alpha-synuclein is a normal cellular process and is enhanced by the familial Parkinson's disease-linked mutations. Proc. Natl. Acad. Sci. U. S. A. 102, 2162–2167. http://dx.doi.org/10.1073/pnas.0406976102.

Luk, K.C., Song, C., O'Brien, P., Stieber, A., Branch, J.R., Brunden, K.R., Trojanowski, J.Q., Lee, V.M.-Y., 2009. Exogenous alpha-synuclein fibrils seed the formation of Lewy body-like intracellular inclusions in cultured cells. Proc. Natl. Acad. Sci. U. S. A. 106, 20051–20056. http://dx.doi.org/10.1073/pnas.0908005106.

Luk, K.C., Kehm, V., Carroll, J., Zhang, B., O'Brien, P., Trojanowski, J.Q., Lee, V.M.-Y., 2012. Pathological-synuclein transmission initiates Parkinson-like neurodegeneration in nontransgenic mice. Science 338, 949–953. http://dx.doi.org/10.1126/science.1227157.

Maroteaux, L., Campanelli, J.T., Scheller, R.H., 1988. Synuclein: a neuron-specific protein localized to the nucleus and presynaptic nerve terminal. J. Neurosci. 8, 2804–2815.

Martin, L.J., Pan, Y., Price, A.C., Sterling, W., Copeland, N.G., Jenkins, N.A., Price, D.L., Lee, M.K., 2006. Parkinson's disease alpha-synuclein transgenic mice develop neuronal mitochondrial degeneration and cell death. J. Neurosci. 26, 41–50. http://dx.doi.org/10.1523/JNEUROSCI.4308-05.2006.

Oueslati, A., Fournier, M., Lashuel, H.A., 2010. Role of post-translational modifications in modulating the structure, function and toxicity of α-synuclein. In: Progress in Brain Research. Elsevier, pp. 115–145.

Peelaerts, W., Bousset, L., Van der Perren, A., Moskalyuk, A., Pulizzi, R., Giugliano, M., Van den Haute, C., Melki, R., Baekelandt, V., 2015. α-Synuclein strains cause distinct synucleinopathies after local and systemic administration. Nature 522, 340–344. http://dx.doi.org/10.1038/nature14547.

Polymeropoulos, M.H., Lavedan, C., Leroy, E., Ide, S.E., Dehejia, A., Dutra, A., Pike, B., Root, H., Rubenstein, J., Boyer, R., Stenroos, E.S., Chandrasekharappa, S., Athanassiadou, A., Papapetropoulos, T., Johnson, W.G., Lazzarini, A.M., Duvoisin, R.C., Di Iorio, G., Golbe, L.I., Nussbaum, R.L., 1997. Mutation in the alpha-synuclein gene identified in families with Parkinson's disease. Science 276, 2045–2047.

Roberts, H., Brown, D., 2015. Seeking a mechanism for the toxicity of oligomeric α-synuclein. Biomol. Ther. 5, 282–305. http://dx.doi.org/10.3390/biom5020282.

Shulman, J.M., De Jager, P.L., Feany, M.B., 2011. Parkinson's disease: genetics and pathogenesis. Annu. Rev. Pathol.: Mech. Dis. 6, 193–222. http://dx.doi.org/10.1146/annurev-pathol-011110-130242.

Singleton, A.B., 2003. Synuclein locus triplication causes Parkinson's disease. Science 302http://dx.doi.org/10.1126/science.1090278. (841–841).

Thayanidhi, N., Helm, J.R., Nycz, D.C., Bentley, M., Liang, Y., Hay, J.C., 2010. Synuclein delays endoplasmic reticulum (ER)-to-Golgi transport in mammalian cells by antagonizing ER/Golgi SNAREs. Mol. Biol. Cell 21, 1850–1863. http://dx.doi.org/10.1091/mbc.E09-09-0801.

Theillet, F.-X., Binolfi, A., Bekei, B., Martorana, A., Rose, H.M., Stuiver, M., Verzini, S., Lorenz, D., van Rossum, M., Goldfarb, D., Selenko, P., 2016. Structural disorder of monomeric α-synuclein persists in mammalian cells. Nature 530, 45–50. http://dx.doi.org/10.1038/nature16531.

Tompkins, M.M., Hill, W.D., 1997. Contribution of somal Lewy bodies to neuronal death. Brain Res. 775, 24–29. http://dx.doi.org/10.1016/S0006-8993(97)00874-3.

Ugalde, C.L., Finkelstein, D.I., Lawson, V.A., Hill, A.F., 2016. Pathogenic mechanisms of prion protein, amyloid-β and α-synuclein misfolding: the prion concept and neurotoxicity of protein oligomers. J. Neurochem. http://dx.doi.org/10.1111/jnc.13772.

Uversky, V.N., Li, J., Bower, K., Fink, A.L., 2002. Synergistic effects of pesticides and metals on the fibrillation of α-synuclein: implications for Parkinson's disease. Neurotoxicology 23, 527–536. http://dx.doi.org/10.1016/S0161-813X(02)00067-0.

Volpicelli-Daley, L.A., Luk, K.C., Patel, T.P., Tanik, S.A., Riddle, D.M., Stieber, A., Meaney, D.F., Trojanowski, J.Q., Lee, V.M.-Y., 2011. Exogenous α-synuclein fibrils induce Lewy body pathology leading to synaptic dysfunction and neuron death. Neuron 72, 57–71. http://dx.doi.org/10.1016/j.neuron.2011.08.033.

Volpicelli-Daley, L.A., Luk, K.C., Lee, V.M.-Y., 2014. Addition of exogenous α-synuclein preformed fibrils to primary neuronal cultures to seed recruitment of endogenous α-synuclein to Lewy body and Lewy neurite–like aggregates. Nat. Protoc. 9, 2135–2146. http://dx.doi.org/10.1038/nprot.2014.143.

Wang, W., Perovic, I., Chittuluru, J., Kaganovich, A., Nguyen, L.T.T., Liao, J., Auclair, J.R., Johnson, D., Landeru, A., Simorellis, A.K., Ju, S., Cookson, M.R., Asturias, F.J., Agar, J.N., Webb, B.N., Kang, C., Ringe, D., Petsko, G.A., Pochapsky, T.C., Hoang, Q.Q., 2011. A soluble-synuclein construct forms a dynamic tetramer. Proc. Natl. Acad. Sci. 108, 17797–17802. http://dx.doi.org/10.1073/pnas.1113260108.

Weinreb, P.H., Zhen, W., Poon, A.W., Conway, K.A., Lansbury, P.T., 1996. NACP, a protein implicated in Alzheimer's disease and learning, is natively unfolded. Biochemistry (Mosc) 35, 13709–13715. http://dx.doi.org/10.1021/bi961799n.

Zarranz, J.J., Alegre, J., Gómez-Esteban, J.C., Lezcano, E., Ros, R., Ampuero, I., Vidal, L., Hoenicka, J., Rodriguez, O., Atarés, B., Llorens, V., Tortosa, E.G., del Ser, T., Muñoz, D.G., de Yebenes, J.G., 2004. The new mutation, E46K, of α-synuclein causes Parkinson and Lewy body dementia: new α-synuclein gene mutation. Ann. Neurol. 55, 164–173. http://dx.doi.org/10.1002/ana.10795.